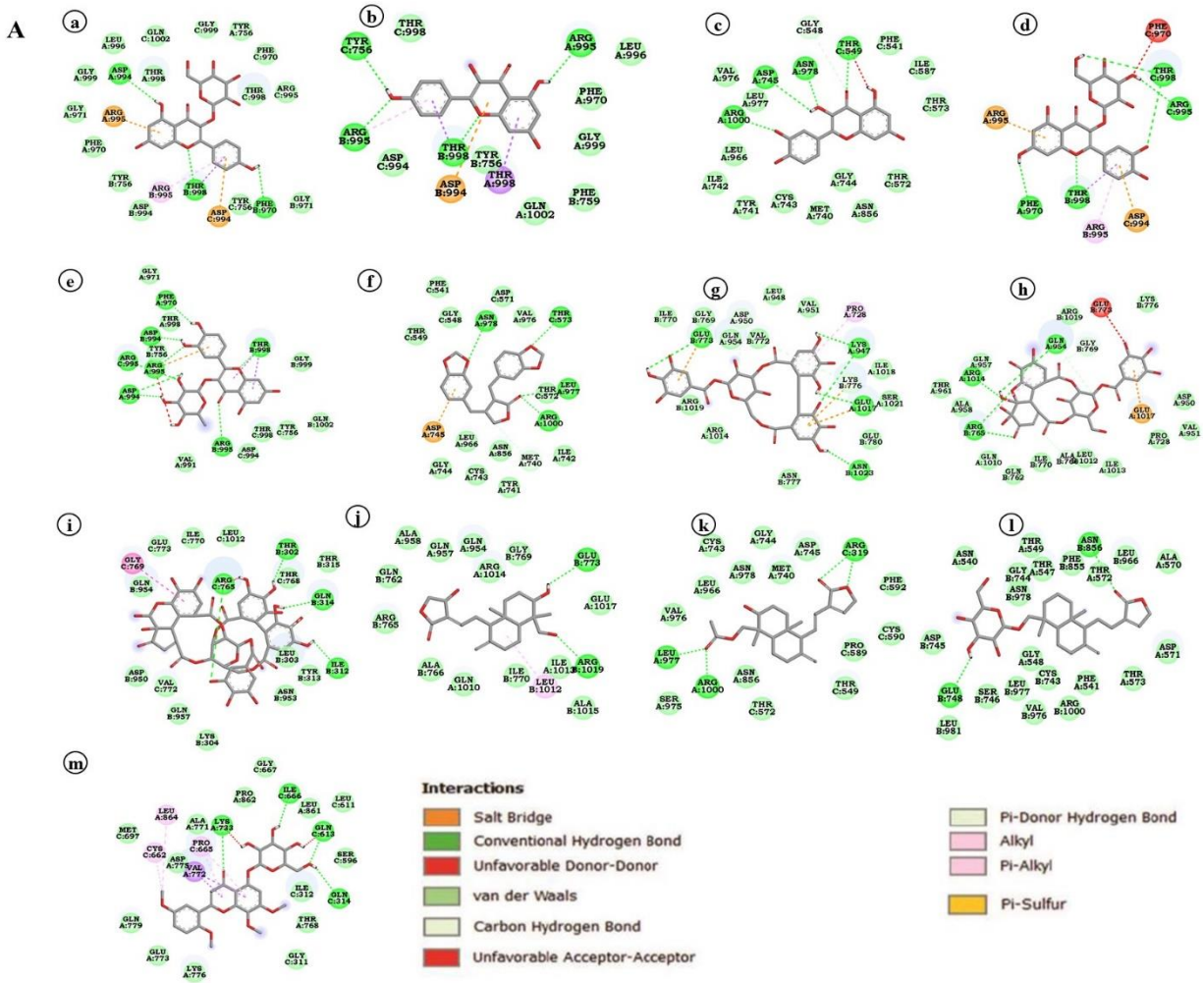
A
a
b
c
d
e
f
g
h
i
j
k
l
m
Interactions
Salt Bridge
Conventional Hydrogen Bond
Unfavorable Donor-Donor
van der Waals
Carbon Hydrogen Bond
Unfavorable Acceptor-Acceptor
Pi-Donor Hydrogen Bond
Alkyl
Pi-Alkyl
Pi-Sulfur

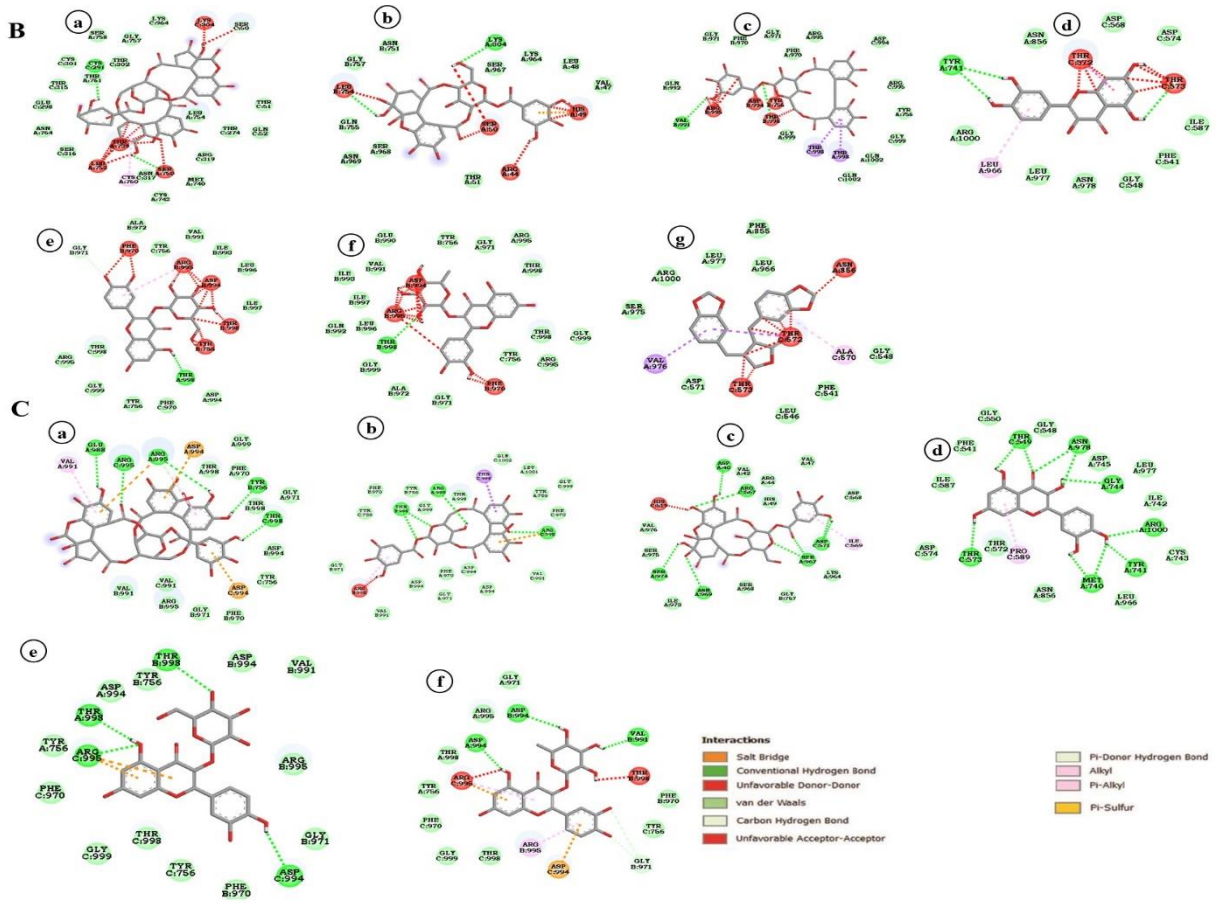
B
a
b
c
d
e
f
g
C
a
b
c
d
e
f
Interactions
Salt Bridge
Conventional Hydrogen Bond
Unfavorable Donor-Donor
van der Waals
Carbon Hydrogen Bond
Unfavorable Acceptor-Acceptor
Pi-Donor Hydrogen Bond
Alkyl
Pi-Alkyl
Pi-Sulfur

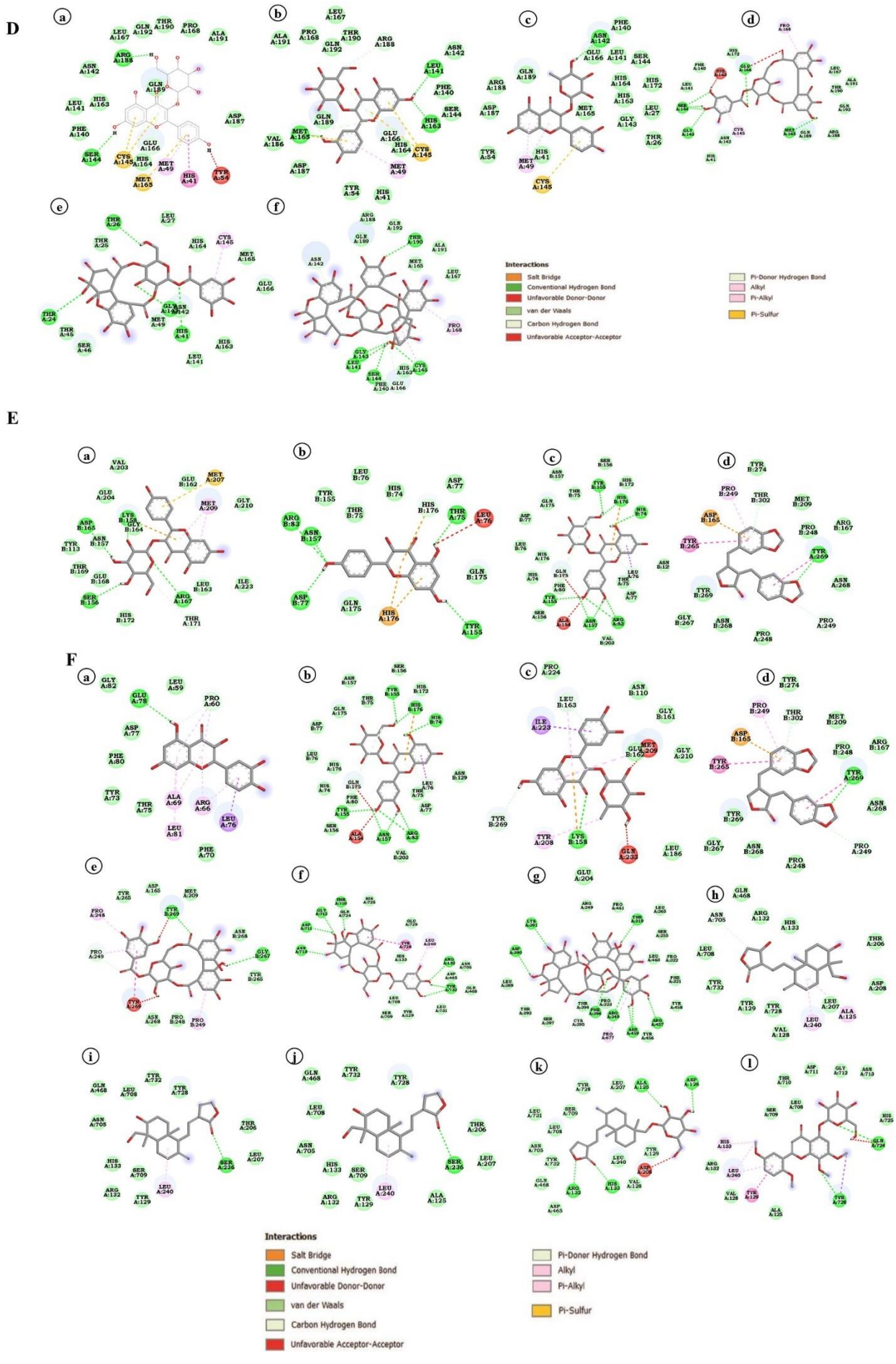
D
a
b
c
d
e
f
Interactions
Salt Bridge
Conventional Hydrogen Bond
Unfavorable Donor-Donor
van der Waals
Carbon Hydrogen Bond
Unfavorable Acceptor-Acceptor
Pi-Donor Hydrogen Bond
Alkyl
Pi-Alkyl
Pi-Sulfur
E
a
b
c
d
F
a
b
c
d
e
f
g
h
i
j
k
l
Interactions
Salt Bridge
Conventional Hydrogen Bond
Unfavorable Donor-Donor
van der Waals
Carbon Hydrogen Bond
Unfavorable Acceptor-Acceptor
Pi-Donor Hydrogen Bond
Alkyl
Pi-Alkyl
Pi-Sulfur

Supplementary figure 1: Hydrogen bond energy is the major contributor in dock score. Hydrogen bond formation between ligand structures and viral receptors is responsible for inhibition of the target protein and it reflects the firmness of bonding between the protein and ligand. The figure represents 2D visualization of interaction between SARS-CoV-2 proteins with phytochemicals from *P. amarus* and *A. paniculata* showing more dock score than remdesivir.

A; S protein (6VSB) with a) astragalin, b) kaempferol c) quercetin d) quercetin-3-O-glucoside e) quercitrin f) hinokinin g) corilagin h) furosin i) geraniin j) isoandrographolide k) 19-O-acetyl-14-deoxy-11,12-didehydroandrographolide l) neoandrographolide m) 5-hydroxy-7,8,2',5'-tetramethoxy flavone

B; S protein (6VXX, closed) a) geraniin b) furosin c) corilagin d) quercetin e) quercetin-3-O-glucoside f) quercitrin g) hinokinin

C; S protein (6YVB, open) a) geraniin b) furosin c) corilagin d) quercetin e) quercetin-3-O-glucoside f) quercitrin

D; 3CLpro (6LU7) with a) astragalin, b) quercetin-3-O-glucoside c) quercitrin, d) corilagin e) furosin f) geraniin

E; PLpro(4OVZ) with a) astragalin, b) kaempferol c) quercetin-3-O-glucoside d) hinokinin

F; RdRp (6NUS) with a) quercetin b) quercetin-3-O-glucoside c) quercitrin d) hinokinin e) corilagin f) furosin g) geraniin, h) isoandrographolide i) 14-deoxy-14,15-didehydroandrographolide j) 14-Deoxyandrographolide k) neoandrographolide l) 5-hydroxy-7,8,2',5'-tetramethoxy flavone

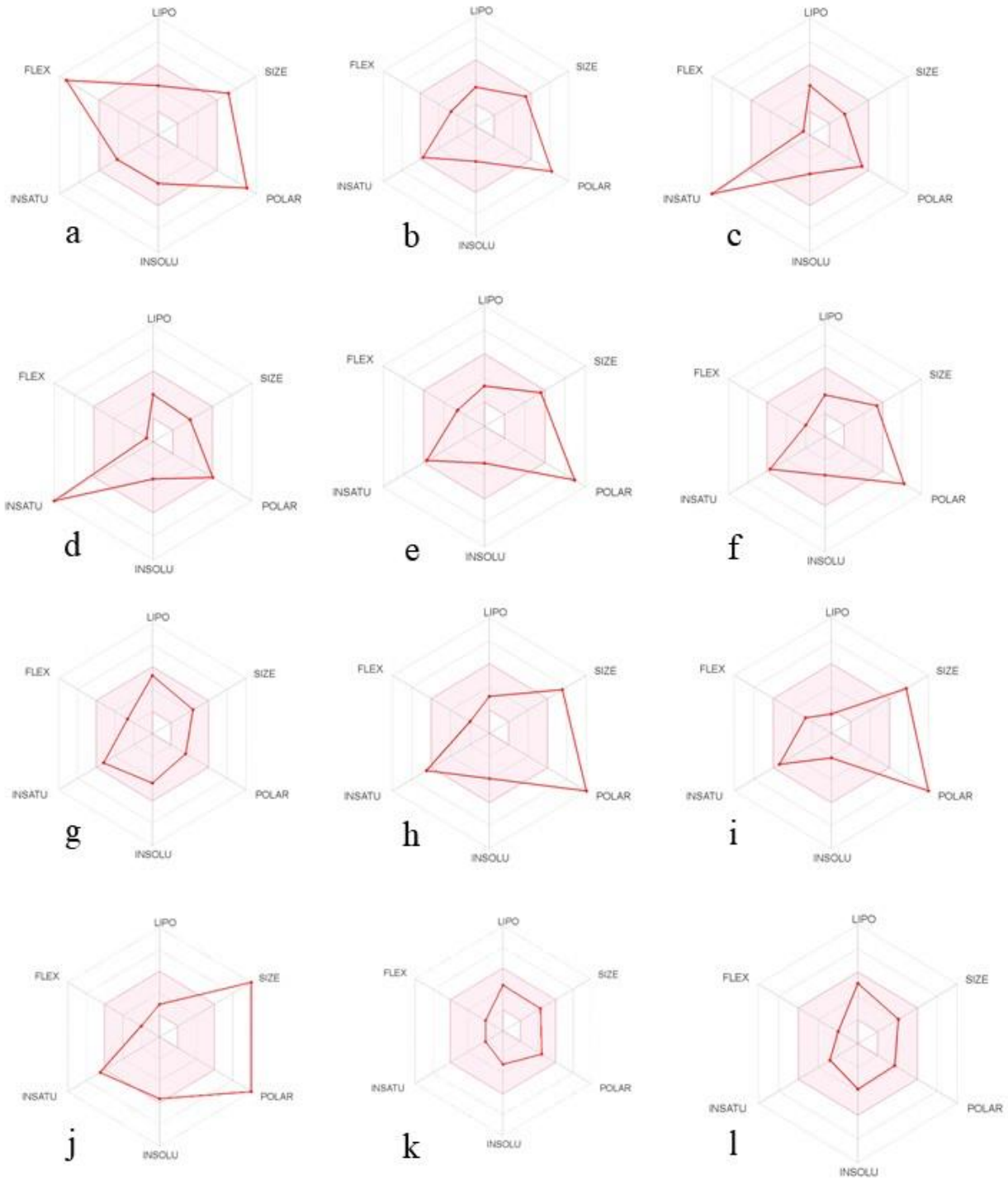
LIPO
SIZE
POLAR
INSOLU
INSATU
FLEX
a
b
c
d
e
f
g
h
i
j
k
l

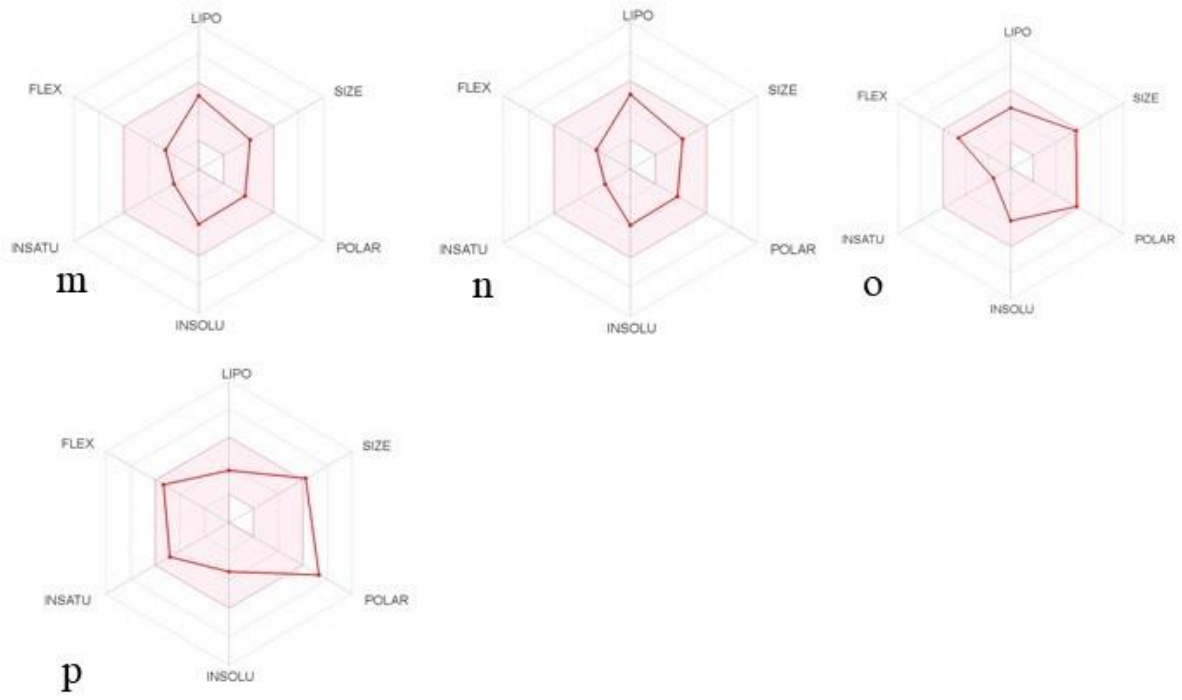

Supplementary figure 2: The pharmacokinetic evaluation and ADME (absorption, distribution, metabolism and excretion) properties predictions of pharmacological compounds in advance are important methods to save huge monetary expenses in drug discovery. The figures a-p represent the ADME properties of selected phytochemicals from *P. amarus* and *A. paniculata.* The coloured zone is the suitable physicochemical space for oral bioavailability. LIPO (Lipophilicity): -0.7 < XLOGP3 < +5.0, SIZE: 150 g/mol < MV < 500 g/mol, POLAR (polarity): 20 $Å^2$ < TPSA < 130 $Å^2$, INSOLU (insolubility): 0 < log S (ESOL) <6, INSATU (insaturation) 0.25 < Fraction Csp3 <1, FLEX (flexibility): 0 < Num. rotatable bonds < 9.

a) Remdesivir, b) Astragalin c) Kaempferol d) Quercetin e) quercetin-3-O-glucoside f) Quercitrin g) Hinokinin h) corilagin i) Furosin j) geraniin k) Isoandrographolide l) 14-deoxy-14,15 didehydroandrographolide m) 14-Deoxyandrographolide n) 19-O-Acetyl-14-deoxy-11,12-didehydroandrographolide o) Neoandrographolide p) 5-hydroxy-7,8,2',5'-tetramethoxy